

Simulating Colliding Flows in SPH with Fractional Derivatives

Oktar Ozgen, Selcuk Sumengen, Marcelo Kallmann,
Carlos FM Coimbra, and Selim Balcisoy

Abstract

We propose a new method based on the use of fractional differentiation for improving the efficiency and realism of simulations based on Smoothed Particle Hydrodynamics (SPH). SPH represents a popular particle-based approach for fluid simulation and a high number of particles is typically needed for achieving high quality results. However, as the number of simulated particles increases, the speed of computation degrades accordingly. The proposed method employs fractional differentiation to improve the results obtained with SPH in a given resolution. The approach is based on the observation that effects requiring a high number of particles are most often produced from colliding flows, and therefore when the modeling of this behavior is improved higher-quality results can be achieved without changing the number of particles being simulated. Our method can be employed to reduce the resolution without significant loss of quality, or to improve the quality of the simulation in the current chosen resolution. The advantages of our method are demonstrated with several quantitative evaluations.

Keywords: fluid simulation, physically-based simulation, fractional derivatives.

1 Introduction

The method of Smoothed Particle Hydrodynamics (SPH) has become a popular particle-based approach for fluid simulation because results incorporating complex interactions (e.g., splashes, coupling, etc.) can be obtained with relatively modest computational complexity [10, 27, 29, 4, 38]. Key to the quality of the results is the determination of an appropriate number of particles achieving sufficient volumetric density. While better results are, in principle, obtained with high concentrations of particles, the computational penalty is significant. Even if specific data structures are used to improve the computation performance, it is always a main concern in practical applications to reduce the computational time while

still obtaining high quality simulation results. This topic is central to the effective implementation of SPH applications, due its suitability to high frame rate interactive applications such as for interactive virtual worlds.

This paper presents a novel approach to address this problem with the introduction of *fractional derivatives* [30] [33] to the SPH equations. The proposed method is able to achieve high quality simulation results with a relatively lower number of particles, achieving results similar to the ones obtained with the higher resolution simulation (see Figure 1).

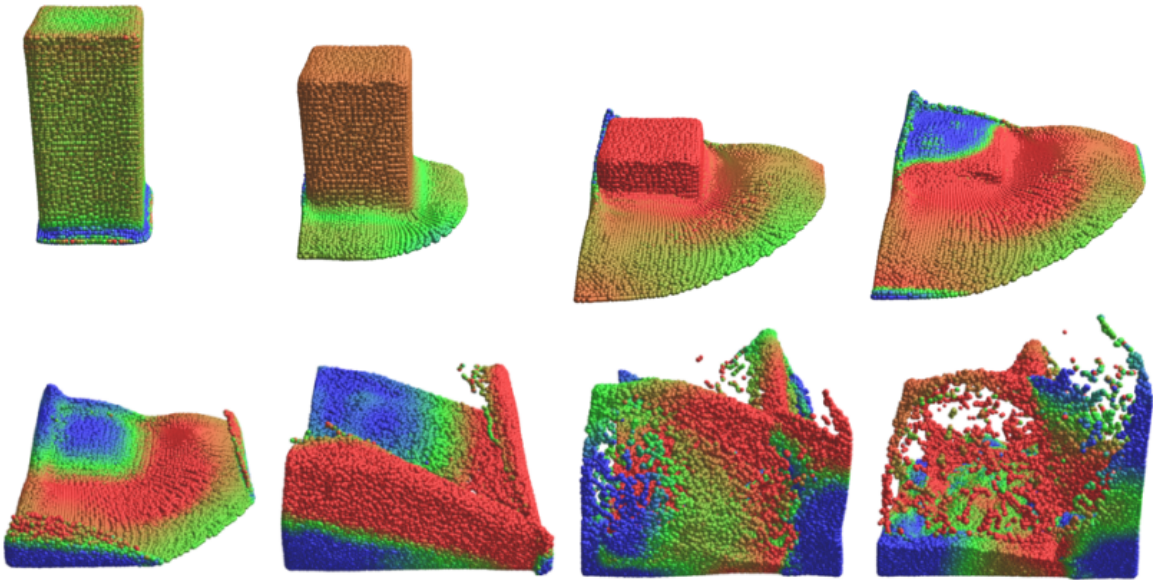


Figure 1: Example of a typical SPH simulation scenario. As demonstrated in several evaluations, our Fractional SPH model will improve the realism of the simulation in a chosen resolution. The colors represent velocity magnitudes in a scale ranging from red (high), to green (medium), and to blue (low).

Our work is based on the observation that in regions of the fluid where the flows do not collide, a lower resolution representation can still correctly represent the fluid because the flows evolve steadily in those regions. However, in regions where the flows collide, the responses to be simulated are higher in number and complexity and a low number of particles will not adequately capture all the occurring phenomena. In these situations, we show that the introduction of a history-laden viscous effect based on fractional forces will restore some of the lost behavior and improve the collision representation, leading to a lower concentration model that yields realistic behavior comparable to the ones obtained with higher concentrations of particles.

It is reasonable to expect that fractional terms can compensate for the loss of information in a particle-based flow and restore the expected behavior of the small volume of water repre-

sented by each particle. Fractional derivatives have been demonstrated to efficiently model memory-laden effects that are observed in immersed particles [9]. The force contributions acting on an oscillating particle immersed in a Newtonian fluid are proportional to: 1) the acceleration of the displaced fluid (the virtual mass force), 2) the velocity of the particle (the Stokes drag), and 3) the so-called history (or Basset) force, which accounts for history effects of the moving flow around the particle. In the limit of infinitesimal particle Reynolds numbers, the formulation including steady Stokes drag, virtual mass and the Basset fractional term is exact. These contributions can be derived directly from the Navier-Stokes equations for the limit of vanishingly small convective effects. Coimbra and Rangel [9] have shown that the Basset force is mathematically equivalent to the half-derivative of the differential velocity between the particle and the far-stream flow. These results indicate that the behavior of immersed particles can be well represented with models based on fractional derivatives. The concept has been well demonstrated by Ozgen et al. [31] on the problem of simulating cloth deformations with underwater behavior.

Our model compensates the loss of information in a lower resolution simulation by adding a half-derivative viscosity in the regions of the flow detected to have significant variations in velocity, a situation that happens in colliding flows. When the simulation is implemented with low concentration of particles, local particle-particle interactions are not enough to correctly depict the flow interactions and memory-laden half-derivatives are used to compensate for the resolution decrease.

2 Background and Related Work

Fluid dynamics governed by Navier-Stokes Equations has been extensively studied in previous years, and several methods have been proposed to numerically solve these equations. In the sections below we first discuss related work in fluid simulation and then provide a background on the related uses of fractional calculus.

2.1 Fluid Simulation

Smoothed Particle Hydrodynamics (SPH) has a long history in physics, developed in 1977 by Gingold and Monaghan [13] to model astrophysical phenomena, and extended to solve many problems in continuum mechanics. There are many uses of particle systems in Computer Graphics, however discrete formulation of continuous fields by particles was first introduced by Desburn et al. [10] for simulating highly deformable bodies. Muller et al. [27] reached very promising results in particle-based fluid simulation for interactive applications

using the SPH method. A very detailed study of SPH since its first emergence is presented by Monaghan [26].

In recent years, new variations to the standard SPH models have also emerged. Solenthaler [38] proposed the PCISPH method for reducing the computation time of standard SPH and increasing the incompressibility of the fluid by employing a prediction-correction scheme based on particle pressures. Raveendran [37] introduced a hybrid approach that uses a Poisson solver along with a local density correction step to increase the stability of SPH method in higher time steps. Solenthaler [2] proposed a two-scale simulation by merging the results from low and high resolution simulations running simultaneously. Adaptive time steps are employed by Ihmsen and Adams [21, 1] in SPH methods to increase the stability of the simulations. SPH applications based on parallel computing are also proposed by various groups [21, 20, 15].

Several researchers have addressed the behavior of fluid flows in Computer Graphics. Elcott et al.[11] modeled the fluid flows by satisfying the conservation of circulation along arbitrary loops. The nature of flows flowing through porous materials is described by Lenaerts et al.[23] with the combination of SPH and the Law of Darcy. The behavior of turbulent fluids is defined using a large-scale numerical solver and physical energy models in Narain[28]. Pfaff et al.[32] handles turbulence around objects immersed in flows by modeling turbulence formation with averaged flow fields. Another interesting work is the study of viscoelastic incompressible fluids in which additional elastic terms are integrated in the Navier-Stokes equations [14]. In Treuille [39], a real-time method for acquiring detailed flows with a small number of basis functions is presented. Our present work contributes to the field by introducing fractional derivatives as a new tool for improving fluid simulations.

2.2 Fractional Calculus and Particle Motion

The subject of Fractional Calculus [30], or the mathematical analysis of differentiation and integration to an arbitrary non-integer order, has recently attracted much interest especially in solid mechanics, rheology, electromagnetism, electrochemistry, and biology.

Fractional Calculus models, aside from their capability of modeling memory-intense and delay systems, have been associated with the exact description of unsteady viscous and viscoelastic phenomena. Coimbra and L'Esperance [8, 24] presented definitive experimental evidence of fractional history effects in the unsteady viscous motion of small particles in suspension. This formulation is exact at low particle Reynolds numbers, but can be extended to include convective effects as illustrated by Pedro et al. [18]. Furthermore, a rich literature is available on the ability of non-integer derivatives to capture non-local behavior and to interpolate between different dynamic regimes [30, 25, 34, 19, 17, 22], including the fundamental modeling of viscoelastic behavior [35] and the unsteady drag for individual

particles moving through a viscous fluid [36].

Stokes was the first to determine the operator Λ_S that relates the force \mathbf{F} acting on a particle to the background flow field \mathbf{U} , such that an expression of the form $\mathbf{F} = \Lambda_S(\mathbf{U})$ is determined. The importance of this discovery was that it allowed for the calculation of the forces acting on the particle by considering only the undisturbed flow conditions as opposed to relating the force to the spatially dependent, non-uniform flow in the vicinity of the particle. Therefore, under special circumstances, it is possible to accurately predict the rate of sedimentation of small particles without ever calculating the flow generated by the motion of the particles [36]. The resulting Stokes drag formula relates the force exerted on the sphere to the constant free-stream velocity \mathbf{U} , the dynamical viscosity of the fluid μ , and the radius a of the sphere in a linear way, given that the particle Reynolds number is maintained much smaller than unity.

Boussinesq [5] and Basset [3] independently extended Stokes' derivation to a case where the particle accelerates through the fluid due to a constant gravitational force but still neglecting the convective terms in the Navier-Stokes equation. The particle equation of motion with a constant forcing (the gravity term) is called the BBO equation.

The BBO equation is an integro-differential equation that has a removable singularity in the integrand of the history term. Coimbra and L'Esperance [8, 24] showed that the history or fractional term can be derived directly from the Stokes operator Λ_S using Duhamel's Superposition Theorem. The history term is found to be simply $a\Lambda_S\nu^{-1/2}D^{1/2}\mathbf{V}$, where ν is the kinematic viscosity of the fluid and $D^{1/2}\mathbf{V}$ represents the half-derivative of the particle velocity [9], which can be computed with the following Riemann-Liouville differential operator:

$$D^{1/2}\mathbf{V} = \frac{1}{\Gamma(1/2)} \int_{-\infty}^t (t - \sigma)^{-1/2} \frac{d\mathbf{V}(\sigma)}{d\sigma} d\sigma, \quad (1)$$

where Γ is the generalized factorial function and $\Gamma(1/2) = \sqrt{\pi}$.

Motivated by these fundamental results on the motion of the particles in unsteady viscous fluids, we aim to increase the physical accuracy of simulating flow collisions in low resolution simulations by utilizing a fractional derivative model. We thus propose a new SPH model with half-derivative viscosity terms to compensate the loss of information in low resolution simulations.

Our proposed model uses history-laden viscous terms that are made proportional to the half-derivative of the relative particle displacements in order to better capture the macroscopic behavior of colliding flows. At first, applying the half-derivative of the differential velocity seems the natural approach to macroscopically account for small volumes of water around the particles in a low resolution SPH simulation, however, the small volumes of water being considered behave differently than a non-fluid particle immersed in the fluid, and the history effects are better described as a viscoelastic effect that can be approximated by a term on the

half-derivative of the displacement [7]. This is akin to describing the macroscopic behavior of a suspension in terms of the behavior of an ensemble of particles. We therefore consider the history effects of interest by applying the half-derivative operator to the relative particle displacements (instead of applying to the relative velocity). The achieved model is able to simulate the different inertial responses among the particles in an efficient way, while capturing the intermediate mechanical behavior between pure elasticity and pure viscosity.

The proposed model is presented in the next section. We then present two experiments that validate the proposed approach by showing that our model generates realistic results in a well-understood fluid simulation scenario and in comparison with an accurate Navier-Stokes solver (Section 4). The following section (Section 5) presents several evaluation results quantifying the improvements obtained in comparison with the standard SPH model. The final sections discuss the results obtained and then conclude the paper.

3 Model

In this section we describe our proposed Fractional SPH model.

3.1 Standard SPH

The Smoothed Particle Hydrodynamics (SPH) model we employ is based on the scheme presented by Muller [27]. SPH is a Lagrangian model where the fluid is represented by a set of particles that carry field attributes. An arbitrary attribute on a given particle's position is computed via smoothing kernels that only consider nearby particles within the core radius h . The smoothing of attributes is modeled with:

$$A_S(r) = \sum_j m_j \frac{A_j}{\rho_j} W(\mathbf{r} - \mathbf{r}_j, h), \quad (2)$$

where m_j is the mass, r_j is the position and ρ_j is the density of a particle j within the core radius h of the smoothing kernel $W(r - r_j, h)$. A_j is the field attribute quantity at r_j .

At each timestep of the simulation, the density values of individual particles are evaluated first:

$$\rho_i = \sum_j m_j W(|\mathbf{r}_i - \mathbf{r}_j|, h), \quad (3)$$

then, the pressure is computed by the ideal gas state equation

$$p = k(\rho - \rho_0), \quad (4)$$

where k is a gas constant and ρ_0 is the rest density. Once the density and the pressure fields are computed, the pressure and viscosity forces acting on particle pairs are computed in a symmetric manner as proposed by Muller [27]:

$$\mathbf{f}_i^{pressure} = - \sum_j m_j \frac{p_i + p_j}{2\rho_j} \nabla W(\mathbf{r}_i - \mathbf{r}_j, h), \quad (5)$$

$$\mathbf{f}_i^{viscosity} = \mu \sum_j m_j \frac{\dot{\mathbf{x}}_j - \dot{\mathbf{x}}_i}{\rho_j} \nabla^2 W(\mathbf{r}_i - \mathbf{r}_j, h), \quad (6)$$

where $\nabla W(\mathbf{r}_i - \mathbf{r}_j, h)$ is the gradient, $\nabla^2 W(\mathbf{r}_i - \mathbf{r}_j, h)$ is the Laplacian of the kernel, μ is the viscosity constant, and finally $\dot{\mathbf{x}}_i = \mathbf{v}_i$ and $\dot{\mathbf{x}}_j = \mathbf{v}_j$ are the velocity vectors of particles i and j respectively.

3.2 Fractional SPH

As discussed in Section 2.2, in order to represent the memory-laden characteristics of the fluid body, we introduce the fractional viscosity term of order 1/2 to the motion of the particles. We achieve this by replacing the first time derivatives of the positions by the half-derivatives of the positions. As a result, the history-based viscosity is defined as:

$$\mathbf{f}_i^{viscosity} = \mu \sum_j m_j \frac{D^{1/2}\mathbf{x}_j - D^{1/2}\mathbf{x}_i}{\rho_j} \nabla^2 W(\mathbf{r}_i - \mathbf{r}_j, h) \quad (7)$$

where $D^{1/2}\mathbf{x}_i$ and $D^{1/2}\mathbf{x}_j$ are the half-derivatives of the positions of particles i and j respectively. Note that the viscosity force is now proportional to the difference of the half-derivatives, achieving the memory-laden viscosity needed to define the motion resulting from flow collisions.

The memory-laden viscosity is especially well suited for fluid phenomena occurring in intense flow collision regions. It is important to observe that in most situations a fluid simulation scenario will contain both regions with flow collisions and regions without any collisions. Our model will improve the quality of the simulation in the regions with flow collisions, which are often the regions producing the most interesting behaviors. Our model will not affect the results obtained in regions with steady flows.

3.3 Computing the Half Derivative Terms

In Coimbra [7], a first-order accurate numerical solution to the history integral of Equation 1 is suggested. Following this solution, the $1/2$ order derivative of \mathbf{x} can be expressed as:

$$\begin{aligned}
D^{1/2}\mathbf{x}_n = & \frac{h}{6\sqrt{\pi}} \sum_{i=1}^{n-1} \left[\frac{\dot{\mathbf{x}}_{i-1}}{(nh - (i-1)h)^{1/2}} \right. \\
& + \left. \frac{2(\dot{\mathbf{x}}_{i-1} + \dot{\mathbf{x}}_i)}{(nh - (i-1/2)h)^{1/2}} + \frac{\dot{\mathbf{x}}_i}{(nh - ih)^{1/2}} \right] \\
& + \frac{0.15h}{\sqrt{\pi}} \left[\frac{\dot{\mathbf{x}}_{n-1}}{h^{1/2}} + \frac{2(\dot{\mathbf{x}}_{n-1} + \dot{\mathbf{x}}_n)}{(0.55h)^{1/2}} + \frac{\dot{\mathbf{x}}_n}{(0.1h)^{1/2}} \right] \\
& + \frac{0.05h}{\sqrt{\pi}} \left[\frac{8\sqrt{2}}{3} \frac{\dot{\mathbf{x}}_n}{(0.05h)^{1/2}} - \frac{4}{3} \frac{\dot{\mathbf{x}}_n}{(0.1h)^{1/2}} \right], \tag{8}
\end{aligned}$$

where h is the timestep, i is the timestep index, and n is the index of the most recent computed timestep. This formulation is also used in Ozgen [31].

In Coimbra [6], a more general and second-order accurate quadrature formula derived using the product trapezoidal method is suggested for derivative orders q in the $0 < q < 1$ range. This fractional-order differential operator reads:

$$D^q\mathbf{x}_n = \frac{h^{1-q}}{\Gamma(3-q)} \sum_{i=0}^n a_{i,n} D^1\mathbf{x}_i, \tag{9}$$

$$a_{i,n} = \begin{cases} (n-1)^{2-q} - n^{1-q}(n+q-2) & \text{if } i = 0, \\ (n-i-1)^{2-q} - 2(n-i)^{2-q} + (n-i+1)^{2-q} & \text{if } 0 < i < n, \\ 1 & \text{if } i = n, \end{cases}$$

where q is the derivative order ($0 < q < 1$), n is the index of the most recently computed timestep, $a_{i,n}$ is the weight of timestep index i at timestep n , and $D^1\mathbf{x}_i = \mathbf{v}_i$ is the velocity of a particle at timestep i . In comparison to the method employed by Ozgen et al. [31], this formulation is relatively simpler and more accurate. In the presented simulations we have used this latter formulation with $q = 0.5$ to acquire the half derivatives.

The fact that computing the half derivative of the position of a particle makes use of all the past velocities of that particle seems to be a computational barrier at first. However, as stated in Ozgen [31], an analysis on the evolution of the weights used for the fractional derivative computation shows that the most recent states have much more influence on the final result of the equation. The plot in Figure 2 shows the evolution of the weights as a function of the

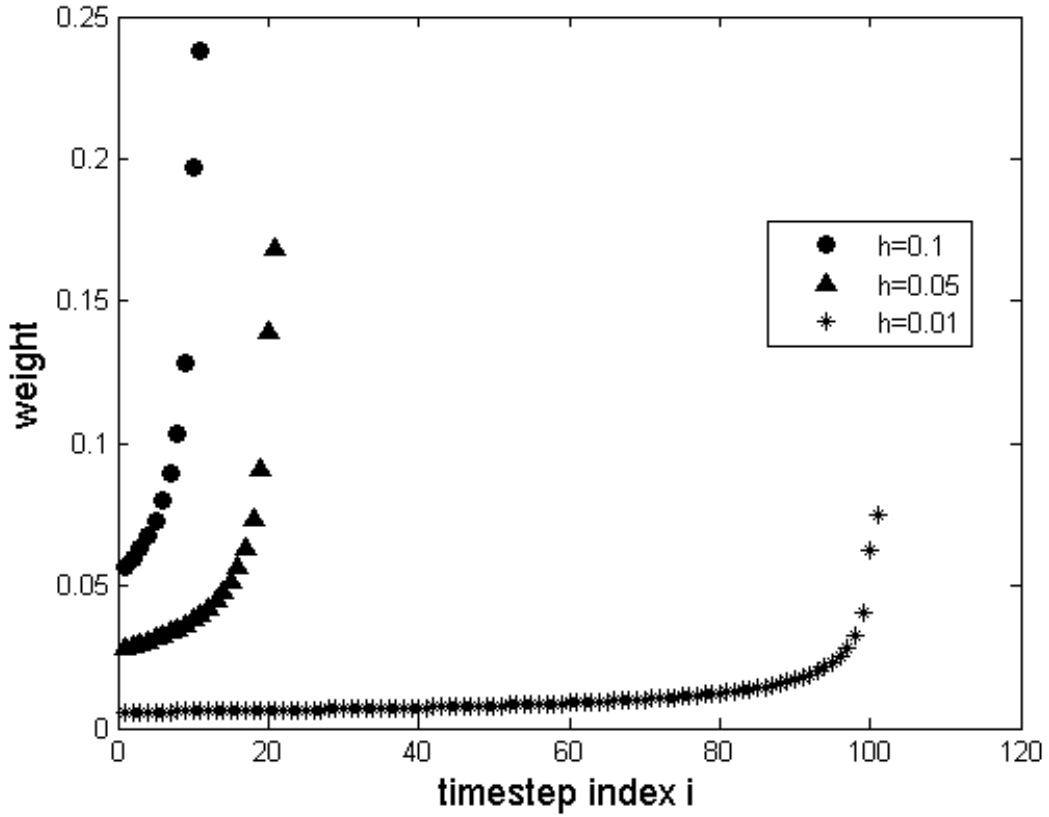


Figure 2: The plot shows how weights rapidly decay as we move away from the most recent timestep.

timestep index i for three different timestep values h . Thus, we only consider the last ten timesteps when computing the half-derivative terms.

4 Validation Experiments

In order to validate the approach taken by our model, we have performed two experiments designed to verify if the results produced by our simulations are in accordance with expected known results. The first experiment simulates a solid sphere in a viscous fluid, and the second experiment simulates the Shear Driven Cavity Test [12].

4.1 Solid Sphere in a Viscous Fluid

L'Esperance et al. [24] describe the experiment where a single small rigid sphere is placed inside a container full of fluid, and the container is then continuously shook by a sinusoidal force. The reason for shaking the container is to create a medium rich in oscillatory flows. The authors state that under certain conditions of particle size, fluid viscosity and oscillation frequency, the Basset history term in the equation of the particle motion becomes dominant. Because the Basset history term can be written in terms of the half-derivative of the particle's velocity [9], the authors show that the recorded path of the sphere in the experiment perfectly matches the solution to the sphere's equation including history effects through the use of fractional derivatives. In the described experiment the trajectory of the sphere will closely match a perfect sinusoidal curve. This provides a ground truth target to achieve with SPH simulations of the experiment, and provides us with an experiment to validate the results produced by our Fractional SPH model.

We have implemented an experimental simulation version of the scenario explained in L'Esperance et al. [24]. We have prepared a 3D fluid simulation of 12K particles, with the fluid located inside a closed rectangular container, and with a solid sphere immersed in the center of the container. The density of the solid sphere was set to be slightly greater than the density of the fluid by increasing the particle's mass by 50% and keeping the particle's volume the same. In the original experiment, the tracked particle was tethered by very thin copper wires to counteract the weight and buoyancy. We achieved the same effect by adjusting the gravity force so that the particle neither sank nor floated. We applied a sinusoidal shaking force to the fluid container, and the fluid was simulated with both standard SPH and our Fractional SPH.

We conducted three different experiments. In the first experiment, we simulated the water flow with the standard SPH model. In the second experiment, we simulated the water with 40% less particles but using our Fractional SPH with history forces included through fractional derivatives. In the last experiment, we simulated the water with the standard SPH in the same resolution of 40% less particles than the high resolution model. The recorded paths of the solid spheres in the three experiments are shown in Figure 3. It can be clearly seen that the inclusion of the history forces improved the results of the low resolution SPH by making the path of the solid sphere closer to the path of the solid sphere in the high resolution SPH. In addition, it can be observed that both the low resolution Fractional SPH and the high resolution SPH generated trajectories that are closer to a perfect sinusoidal curve.

We also obtain an indication that SPH simulations can reproduce fluid behaviors as they occur in real life and that by increasing its resolution we can improve the obtained results. This can be noticed by observing that the high resolution SPH experiment produces a curve (blue curve) that looks closer in shape to a well-defined sinusoidal shape than the low resolution SPH experiment (red curve). Therefore, it is reasonable to evaluate our proposed

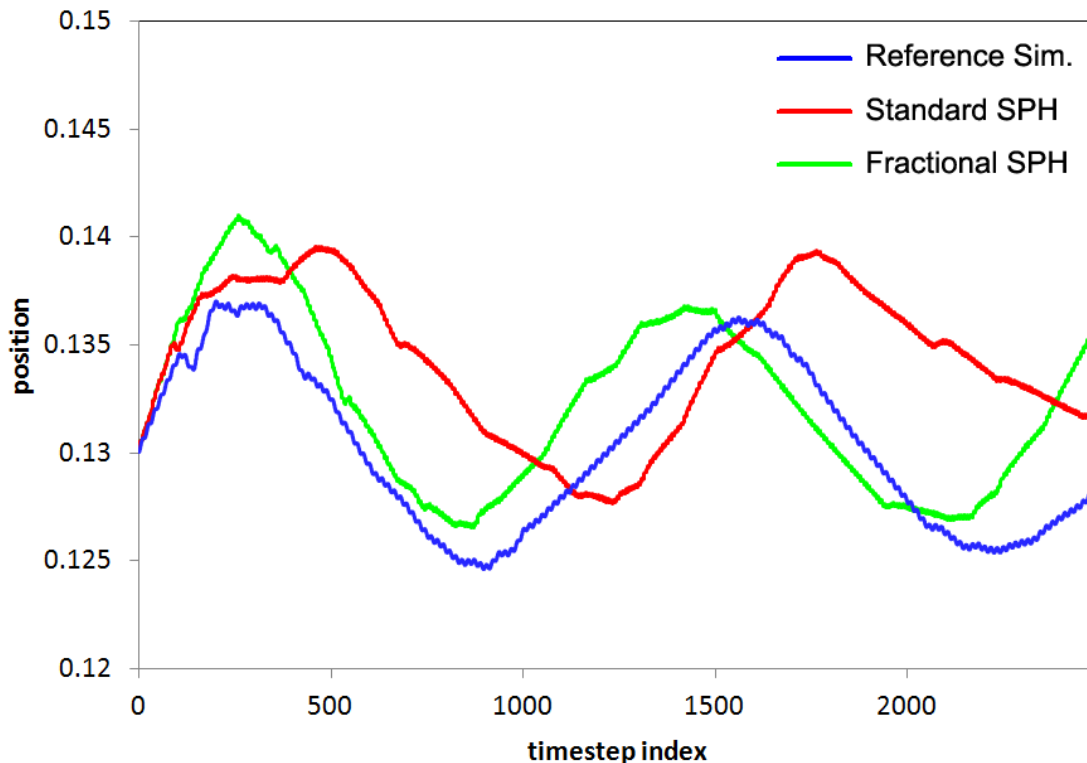


Figure 3: The figure shows the path followed by the solid sphere located in a fluid container subjected to a continuous sinusoidal shaking force. The blue, red and green curves show the path of the sphere in a fluid simulated with high resolution standard SPH, low resolution standard SPH and low resolution Fractional SPH, respectively.

method by applying it at a given resolution and then comparing the results obtained against a higher resolution standard SPH simulation. We will adopt this comparison strategy in the evaluation experiments of Section 5. These preliminary experiments also indicate that the addition of fractional terms is beneficial and that higher resolutions in SPH will lead to improved behaviors. These results provide reasonable validation of our proposed approach.

4.2 Shear Driven Cavity Test

Our second validation experiment employed a standard test known as the Shear Driven Cavity Test (or Lid Driven Cavity Test) in Fluid Dynamics [12]. In this test, flow is generated by moving the top wall of a square box full of fluid while the other three walls are stationary. The top wall of the box moves in the horizontal direction with a constant speed, and the flow reaches a steady state after running the simulation for a while.

We implemented this test with our standard and Fractional SPH implementations, with various number of particles and Reynolds number values. All tests demonstrated that our Fractional SPH model produced results closely matching the results computed by a high-precision fluid solver. We compared our results against the results generated by OpenFOAM, a grid-based solver widely employed by the CFD community [16]. One example of the obtained results are demonstrated in Figure 4. As it can be seen in the figure, standard SPH and Fractional SPH simulations with 40K particles follow the grid-based solution tightly, showing that the viscosity behavior of both fluids are valid and that the use of fractional derivatives in the viscosity formulation does not introduce any additional viscosity to the standard formulation. These results were computed with the simulations on the steady state phase. These results are important to demonstrate that the Fractional SPH model also performs well in steady flow cases. Our model will thus not degrade the results obtained in regions without colliding flows.

5 Evaluation Experiments

In order to quantify the improvements obtained with our Fractional SPH model we have designed a simulation scenario based on a rectangular grid that is rich in flow collisions. We placed several force sources that continuously run and create flows moving towards opposite directions and colliding at several regions. Several evaluations were then performed by comparing low-resolution Fractional and standard SPH simulations against the corresponding higher resolution standard SPH simulation. As validated in the previous section, we consider the high-resolution standard SPH simulation to be the reference simulation for our comparisons. The low-resolution simulation that generated less error against the high-resolution simulation was considered to be physically more accurate. In these experiments we used explicit Euler numerical integration.

We discretized a 2D fluid grid by placing 48 equally distributed grid points. Our 2D grid scenario was borderless and cyclic, meaning that the particles penetrating a particular wall will come back to the scene from the opposite wall. Keeping all the initial conditions the same, we conducted three different simulations with this scenario. The first simulation was a high resolution standard SPH with 1500 particles. This one was considered to be the reference simulation. The second simulation was a low resolution standard SPH with 1250 particles and the third simulation was a low resolution Fractional SPH with 1250 particles. As expected, our Fractional SPH model has showed to generate much less error rates than standard SPH at the regions with intense flow collisions. We measured the average velocity vectors of 48 different circular regions centered at the grid points. The average velocity of a circular region for a given timestep is calculated by averaging the angular difference of the velocities of all particles within that region at that timestep. The placement of source forces,

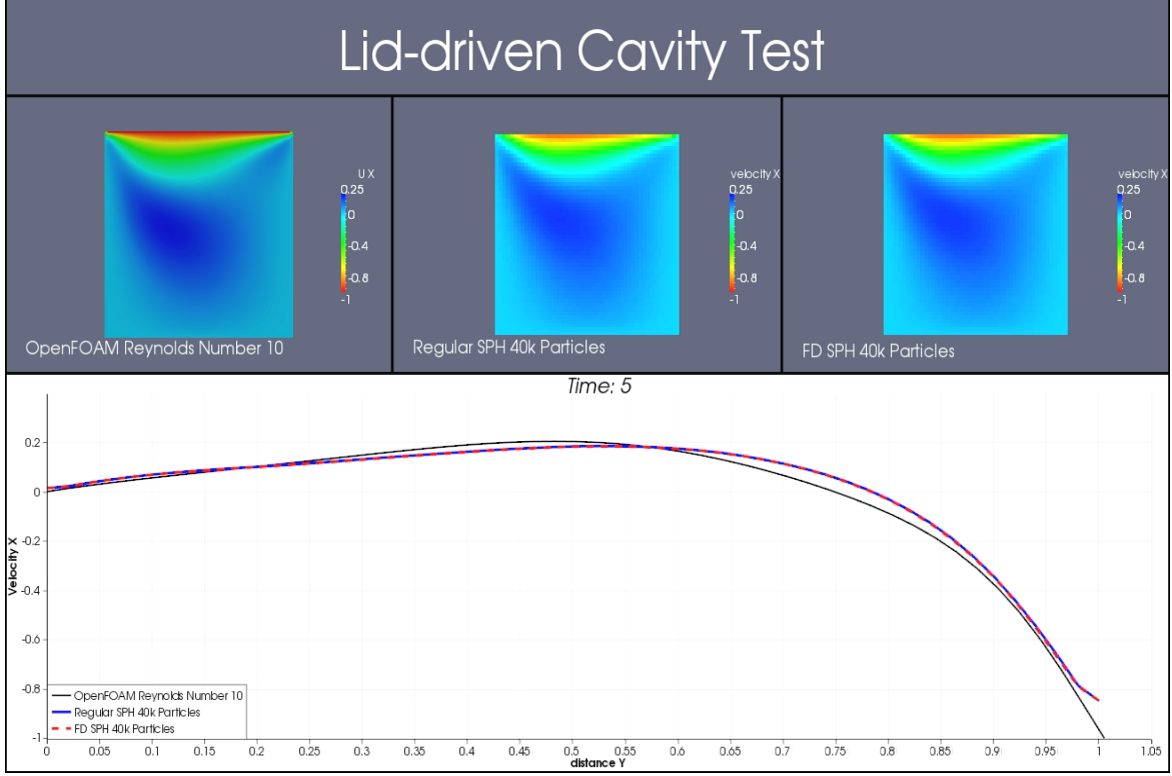


Figure 4: Lid-driven cavity test comparing OpenFOAM’s grid-based Navier-Stokes solution (black curve), standard SPH (blue curve) and Fractional SPH (dashed red curve) with 40k particles. The velocities along the vertical line $x = 0.5$ passing by the center of the box are demonstrated at $t = 5s$ when the simulations are in steady state. The horizontal axis in the graph represents the vertical coordinates along the line $x = 0.5$. The similarity of the curves validate the viscosity behavior of the Fractional SPH simulation in a steady flow scenario.

measurement regions, and the shape of the grid is presented in Figure 5.

The angular difference of the average velocity vectors of each region was first computed for every timestep, then, for all the regions, we took the average of the angular errors by dividing the error sum to the total number of timesteps. The average error that each region produces with respect to the high resolution simulation was obtained with:

$$\epsilon_j = \sum_{i=1}^n \frac{1}{n} \arccos \left(\frac{\mathbf{v}^{j i_{SE}} \cdot \mathbf{v}^{j i_{SHR}}}{|\mathbf{v}^{j i_{SE}}| |\mathbf{v}^{j i_{SHR}}|} \right), \quad (10)$$

where ϵ_j is the average error generated at region j , i is the timestep index, n is the total number of timesteps, and $\mathbf{v}^{j i_{SE}}$ and $\mathbf{v}^{j i_{SHR}}$ are the average velocities of region j at timestep

i , for the evaluated simulation SE and the high resolution simulation SHR , respectively.

With this scheme, we are able to compare the number of grid regions that performed better with each SPH formulation. The method that resulted with more successful grid regions is considered to perform better overall. The next section presents and discusses in detail the results obtained. Additional results with 3D simulations are also presented.

6 Results and Discussion

We first analyze the results presented in Figure 5. The arrows show the placement and the direction of force sources and the circles indicate the 48 comparison regions. The color range is between red and green. The color red shows that standard SPH is producing less error and the green shows that Fractional SPH is producing less error. The yellow regions are the ones where both simulations create almost the same error rates. As demonstrated in this figure, the regions where flows collide tend to be green most of the time. This indicates that the fluid behavior that emerges from intense flow collisions is better modeled by Fractional SPH. The yellow regions are where few flow collisions occur and flows mostly tend to move to a fixed direction. As expected, no significant differences exist between the two simulations on these regions. The few orange regions where Fractional SPH is performing slightly worse than the standard SPH are always located near the force sources. These regions produce slightly worse error rates because they have always relatively less particles in them, due the fact that the continuous flows are generated from these regions. The lack of enough particles in these regions leads to a less accurate error measurement.

Figure 6 presents the comparison of angular error rates (in radians) of regional velocities, generated by both standard SPH and Fractional SPH, at a region rich in flow collisions, over the course of 500 timesteps. As can be observed, the error rate tends to be small at the beginning because of the same initial positions of the particles. However, the Fractional SPH produces less error than standard SPH as the simulation progresses.

Figure 7 shows the same results on a different region of the grid. This region is on the middle right of the grid and it is poor in flow collisions. As can be seen on the graph, the difference between the error rates generated between standard and Fractional SPH tend to decrease on this kind of regions. This result is expected in the sense that the difference of velocities of two particles moving towards the same direction with similar speed causes the viscosity to vanish.

Aside from comparing the direction of regional velocities, we also compared the evolution of velocity magnitudes on each region over the course of 500 timesteps. As it was the case for velocity directions, velocity magnitudes tend to be more similar to the high resolution simulation in Fractional SPH than standard SPH. Figure 8 shows the velocity magnitudes of

a region rich in flow collisions, which is placed in the middle of the grid, for 3 simulations. The blue line is the high resolution reference simulation, the red line is the standard SPH and the green line is the Fractional SPH. As can be observed, Fractional SPH is better approximating the high resolution simulation. Figure 9 shows that the difference between the effects of standard and Fractional SPH is minimized on regions poor in flow collisions.

We have also experimented with 3D SPH simulations following the same flow scenario but with the border of the fluid grid acting like walls. We used 12K particles for the high resolution reference simulation. We increased the gap between high and low resolution fluids by only using 3K particles for low resolution simulations. The same comparison scheme is employed to compare the simulations and calculate the error rates. The time of evaluation was extended to 1000 timesteps in order to have a wider comparison window.

Figure 10 and Figure 11 show the error produced by regional velocity directions and magnitudes, respectively. The comparisons were conducted at a region rich in flow collisions, over the course of 1000 timesteps. As can be observed in the figures, our method produces less error than the standard SPH in 90% of the timesteps.

In terms of performance, our method runs real-time for simulations with up to 5k particles and runs with 4 FPS for simulations with 20k particles on AMD Athlon II X4 3.2 GHz computer. The use of half derivatives in the SPH implementation does not affect the complexity or the running time of the algorithm. In Equation 9, the weights are always calculated based on the terms q and $n - i$. The value of q must always be equal to 0.5 to acquire the half derivatives. Given that we only use the ten most recent terms of the history terms, $n - i$ terms always stay the same for all the ten weights, except for the first ten timesteps. Because Equation 9 makes use of the past particle velocities, we require some extra memory space to store the previous velocities. Therefore, the weights can be precomputed and used in combination with pre-recorded velocities.

Fractional SPH also proved itself useful by allowing larger timesteps in the integration. It was observed that our Fractional SPH simulations were more stable than standard SPH when using large timesteps especially for viscous fluids. In Figure 12, standard SPH and Fractional SPH simulations are compared for different sizes of timesteps. Fractional SPH allowed 2 times larger timesteps, while standard SPH becomes unstable after a small increase. We also noticed that our method performed better in the early stages of the Shear Driven Cavity test, when the flows were not stabilized yet. This was observed in the 3D version of Shear Driven Cavity test and some results are presented in Figure 13. Additional examples demonstrating 3D simulations with our Fractional model are presented in Figure 14.

In summary, we demonstrate that Fractional SPH always produces better results than the standard SPH in regions where flow collisions are detected. Both in 2D and 3D simulations, our Fractional SPH model produced less error on 73% of our grid regions, in comparison with the standard SPH. Note that this percentage depends directly on the density of colliding

flows on the scene. A scenario with more colliding flows will definitely increase the success rate of Fractional SPH. The videos accompanying this submission provide additional examples and results.

7 Conclusions

We have introduced a new methodology for fluid simulation based on the use of Fractional Calculus with Smoothed Particle Hydrodynamics. We have demonstrated in several experiments that our method can better simulate observed fluid behavior emerging from flow collisions. The fact that the memory-laden viscosity terms modeled by fractional derivatives are able to increase the accuracy of low resolution SPH simulations is promising as a technique to improve the quality and computational efficiency of SPH.

Acknowledgements

Selcuk Sumengen was funded by TUBITAK (BIDEB 2214) during his visit to University of California, Merced between September 2009 and February 2010.

References

- [1] Adams, B., Pauly, M., Keiser, R., Guibas, L.J.: Adaptively sampled particle fluids p. 48 (2007)
- [2] Barbara, S., Gross, M.: Two-scale particle simulation. *ACM Transactions on Graphics (Proc. SIGGRAPH)* **30**(4), 81:1–81:8 (2011)
- [3] Basset, A.B.: On the motion of a sphere in a viscous liquid. *Transactions of the Royal Philosophy Society of London* (179), 43–63 (1888)
- [4] Becker, M., Teschner, M.: Weakly compressible sph for free surface flows. In: *SCA '07: Proceedings of the 2007 ACM SIGGRAPH/Eurographics symposium on Computer animation*, pp. 209–217. Eurographics Association, Aire-la-Ville, Switzerland, Switzerland (2007)
- [5] Boussinesq, J.: Sur la résistance qu'oppose un liquide indéfini en repos, sans pesanteur, au mouvement varié d'une sphère solide qu'il mouille sur toute sa surface, quand les vitesses restent bien continues et assez faibles pour que leurs carrés et produits soient négligeables. *C. R. Acad. Sci.* pp. 935–937 (1885)

- [6] C.M. Soon C.F.M. Coimbra, M.K.: The variable viscoelasticity oscillator. *Annalen der Physik* (14), 378–389 (2005)
- [7] Coimbra, C.: Mechanics with variable order operators. *Annalen der Physik* (12), 692–703 (2003)
- [8] Coimbra, C., L’Esperance, D., Lambert, A., Trolinger, J., Rangel, R.: An experimental study on the history effects in high-frequency Stokes flows. *Journal of Fluid Mechanics* (504), 353–363 (2004)
- [9] Coimbra, C., Rangel, R.: General solution of the particle equation of motion in unsteady Stokes flows. *Journal of Fluid Mechanics* (370), 53–72 (1998)
- [10] Desbrun, M., Gascuel, M.P.: Smoothed particles: a new paradigm for animating highly deformable bodies pp. 61–76 (1996)
- [11] Elcott, S., Tong, Y., Kanso, E., Schröder, P., Desbrun, M.: Stable, circulation-preserving, simplicial fluids. *ACM Trans. Graph.* **26**(1), 4 (2007)
- [12] G. R. Liu, M.B.L.: *Smoothed Particle Hydrodynamics: A Meshfree Particle Method*. World Scientific Publishing Company (2003)
- [13] Gingold, R.A., Monaghan, J.J.: Smoothed particle hydrodynamics - theory and application to non-spherical stars. *Royal Astronomical Society* **181**, 375–389 (1977)
- [14] Goktekin, T.G., Bargeil, A.W., O’Brien, J.F.: A method for animating viscoelastic fluids. In: *SIGGRAPH ’04: ACM SIGGRAPH 2004 Papers*, pp. 463–468. ACM, New York, NY, USA (2004)
- [15] Harada, T., Koshizuka, S., Kawaguchi, Y.: Smoothed particle hydrodynamics on gpus. *Structure* pp. 1–8 (2007). URL <http://individuals.iii.u-tokyo.ac.jp/yoichiro/report/report-pdf/harada/international/2007cgi.pdf>
- [16] Henry Weller, C.G.: *Openfoam* (2010)
- [17] Hilfer, R.: *Applications of Fractional Calculus in Physics*. World Scientific, River Edge, NJ (2000)
- [18] H.T.C. Pedro M.H. Kobayashi, J.P., Coimbra, C.: Variable order modeling of diffusive-convective effects on the oscillatory flow past a sphere. *Journal of Vibration and Control* **14**, 1569–1672 (2008)
- [19] Hu, Y.: Integral transformations and anticipative calculus for fractional brownian motions. In: *Memoirs of the American Mathematical Society* (2005)
- [20] Ihmsen, M., Akinci, N., Becker, M., Teschner, M.: A parallel sph implementation on multi-core cpus. *Computer Graphics Forum* **0**(0), 1–12 (2011)

- [21] Ihmsen, M., Akinci, N., Gissler, M., Teschner, M.: Boundary handling and adaptive time-stepping for pcisph. In: VRIPHYS, pp. 79–88 (2010)
- [22] Kilbas, A., Srivastava, H., Trujillo, J.: Theory and Applications of Fractional Differential Equations. Amsterdam, The Netherlands (2006)
- [23] Lenaerts, T., Adams, B., Dutré, P.: Porous flow in particle-based fluid simulations. In: SIGGRAPH '08: ACM SIGGRAPH 2008 papers, pp. 1–8. ACM, New York, NY, USA (2008)
- [24] L'Esperance, D., Coimbra, C., Trolinger, J., Rangel, R.: Experimental verification of fractional history effects on the viscous dynamics of small spherical particles. *Experiments in Fluids* (38), 112–116 (2005)
- [25] Miller, K., Ross, B.: An Introduction to the Fractional Calculus and Fractional Differential Equations. John Wiley and Sons, New York, NY (1993)
- [26] Monaghan, J.J.: Smoothed particle hydrodynamics. *Reports on Progress in Physics* **68**(8), 1703 (2005). URL <http://stacks.iop.org/0034-4885/68/i=8/a=R01>
- [27] Müller, M., Charypar, D., Gross, M.: Particle-based fluid simulation for interactive applications. In: SCA '03: Proceedings of the 2003 ACM SIGGRAPH/Eurographics symposium on Computer animation, pp. 154–159. Eurographics Association, Aire-la-Ville, Switzerland, Switzerland (2003)
- [28] Narain, R., Sewall, J., Carlson, M., Lin, M.C.: Fast animation of turbulence using energy transport and procedural synthesis. In: SIGGRAPH Asia '08: ACM SIGGRAPH Asia 2008 papers, pp. 1–8. ACM, New York, NY, USA (2008)
- [29] Oger, G., Doring, M., Alessandrini, B., Ferrant, P.: An improved sph method: Towards higher order convergence. *J. Comput. Phys.* **225**(2), 1472–1492 (2007)
- [30] Oldham, K., Spanier, J.: The Fractional Calculus. Academic Press, New York, NY (1974)
- [31] Ozgen, O., Kallmann, M., Ramirez, L., Coimbra, C.: Underwater cloth simulation with fractional derivatives. *ACM Transactions on Graphics (TOG)* **29**(3), 1–9 (2010)
- [32] Pfaff, T., Thuerey, N., Selle, A., Gross, M.: Synthetic turbulence using artificial boundary layers. In: SIGGRAPH Asia '09: ACM SIGGRAPH Asia 2009 papers, pp. 1–10. ACM, New York, NY, USA (2009)
- [33] Podlubny, I.: Fractional Differential Equations. Academic Press, London, UK (1999)
- [34] Podlubny, I.: Fractional Differential Equations. Academic Press, San Diego, CA (1999)

- [35] Ramirez, L., Coimbra, C.: A variable order constitutive relation for viscoelasticity. *Annalen der Physik* **16,7-8**, 543–552 (2007)
- [36] Ramirez, L., Coimbra, C.: On the variable order dynamics of the nonlinear wake caused by a sedimenting particle. *Physica D* **240,13**, 1111–1118 (2011)
- [37] Raveendran, K., Wojtan, C., Turk, G.: Hybrid smoothed particle hydrodynamics. In: *Proceedings of the 2011 ACM SIGGRAPH/Eurographics Symposium on Computer Animation, SCA '11*, pp. 33–42. ACM, New York, NY, USA (2011)
- [38] Solenthaler, B., Pajarola, R.: Predictive-corrective incompressible sph. In: *SIGGRAPH '09: ACM SIGGRAPH 2009 papers*, pp. 1–6. ACM, New York, NY, USA (2009)
- [39] Treuille, A., Lewis, A., Popović, Z.: Model reduction for real-time fluids. In: *ACM SIGGRAPH 2006 Papers*, pp. 826–834. ACM, New York, NY, USA (2006)

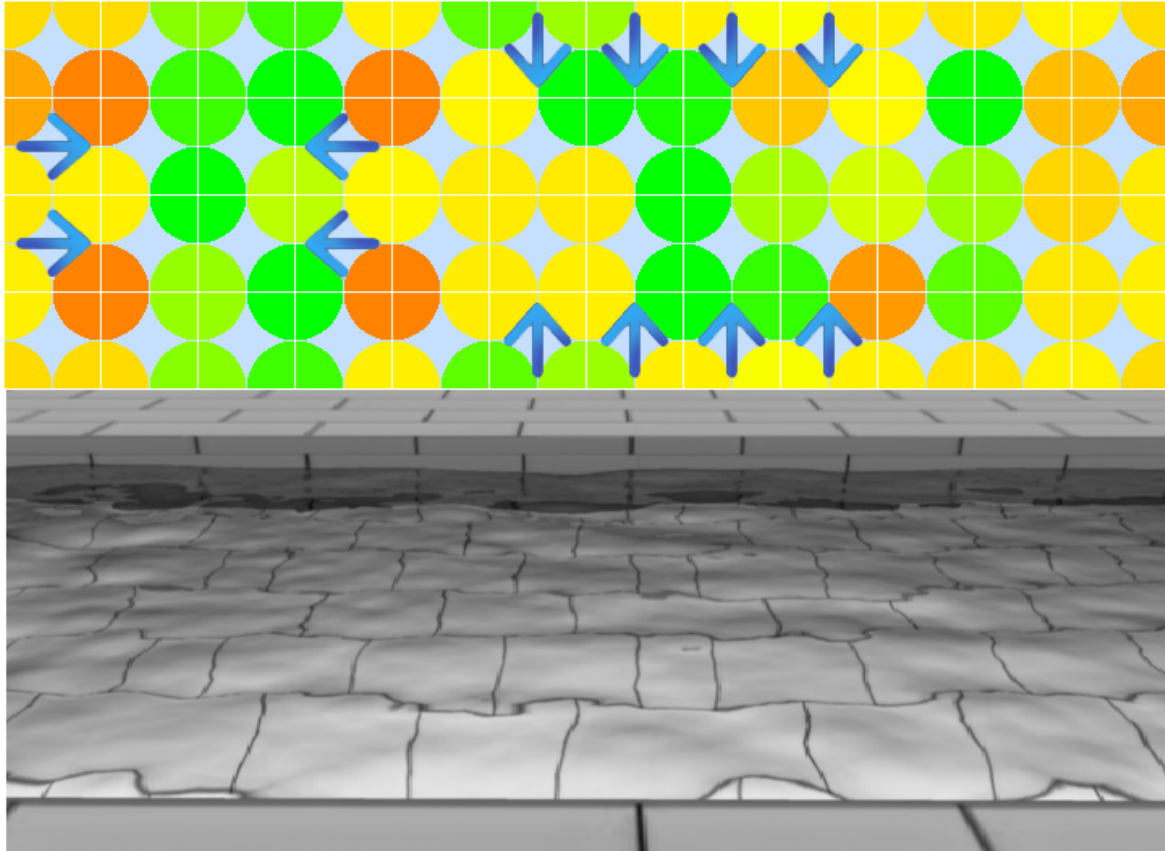


Figure 5: Simulation scheme (top image) and its corresponding fluid simulation scenario (bottom image). The simulation scheme shows both the flow generation configuration and the results of our experiments. The arrows show the force sources creating the flows. The circles show the regions where we computed the average velocity directions in order to quantitatively compare the simulations. The colors are in the red-green range and represent the difference of angular velocity error rates produced by the low resolution standard SPH and low resolution Fractional SPH when compared against the higher resolution standard SPH. Our Fractional SPH method performs better than the standard SPH in the green regions, the difference is similar in yellow regions, and our method performs slightly worse in the orange regions.

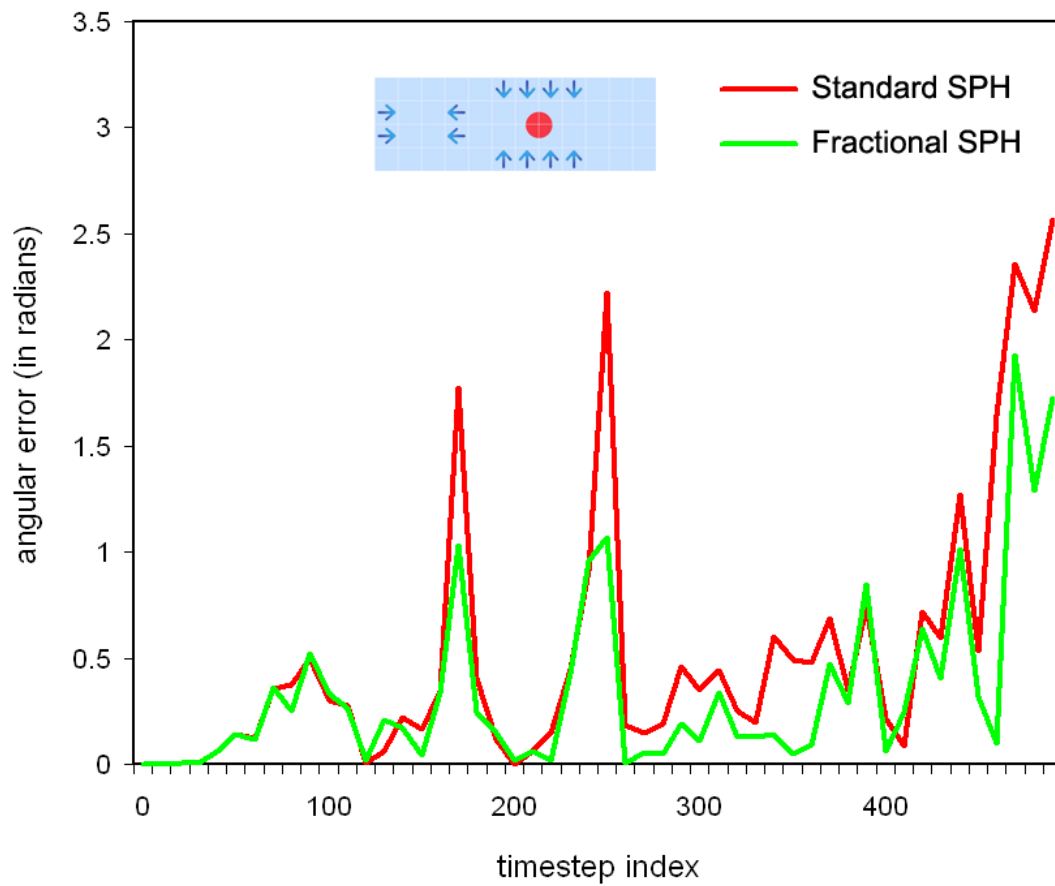


Figure 6: The plot shows the error rates in velocity directions of the region marked with the red disc, over 500 timesteps of simulation. The red and green lines represent the simulations of low resolution standard SPH and low resolution Fractional SPH compared against higher resolution standard SPH. The region marked with the red disc is rich in flow collisions.

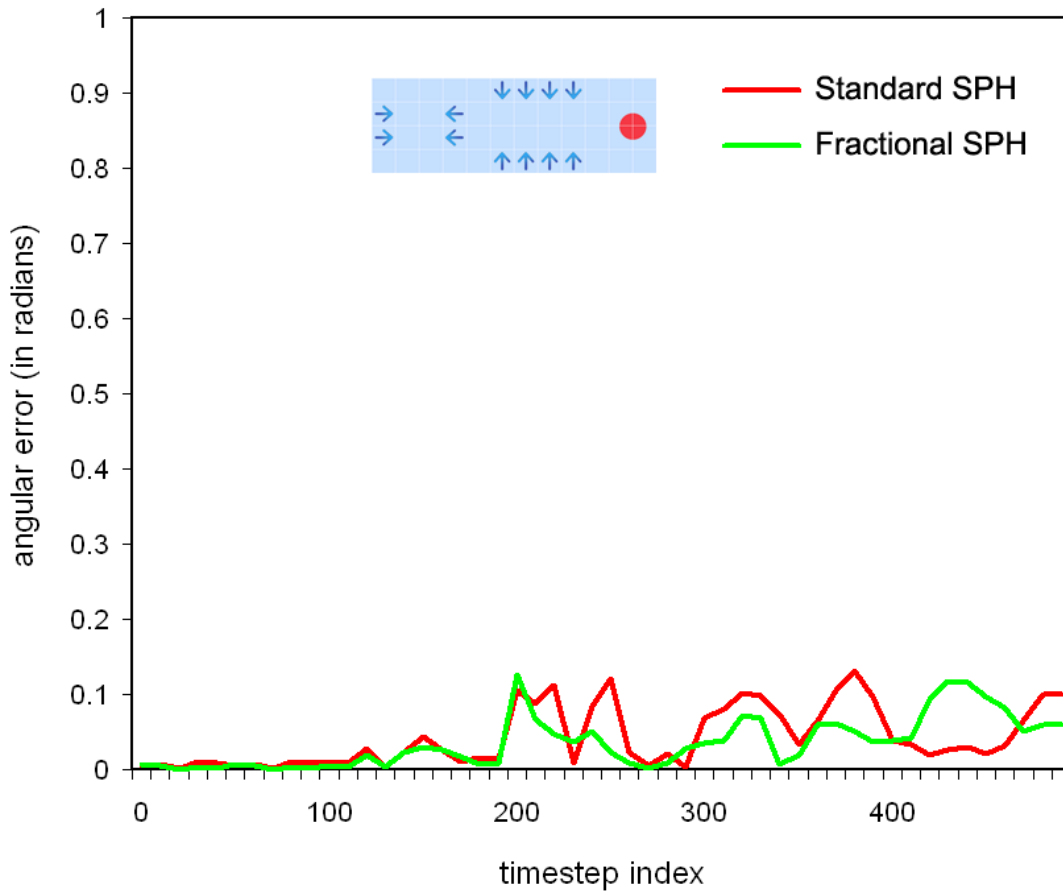


Figure 7: The plot shows the error rates in velocity directions of the region marked with the red disc, over a simulation of 500 timesteps, for 2D simulations. The red and green lines represent the simulations of low resolution standard SPH and low resolution Fractional SPH compared against higher resolution standard SPH, respectively. Here the region marked with red disc is poor in flow collisions.

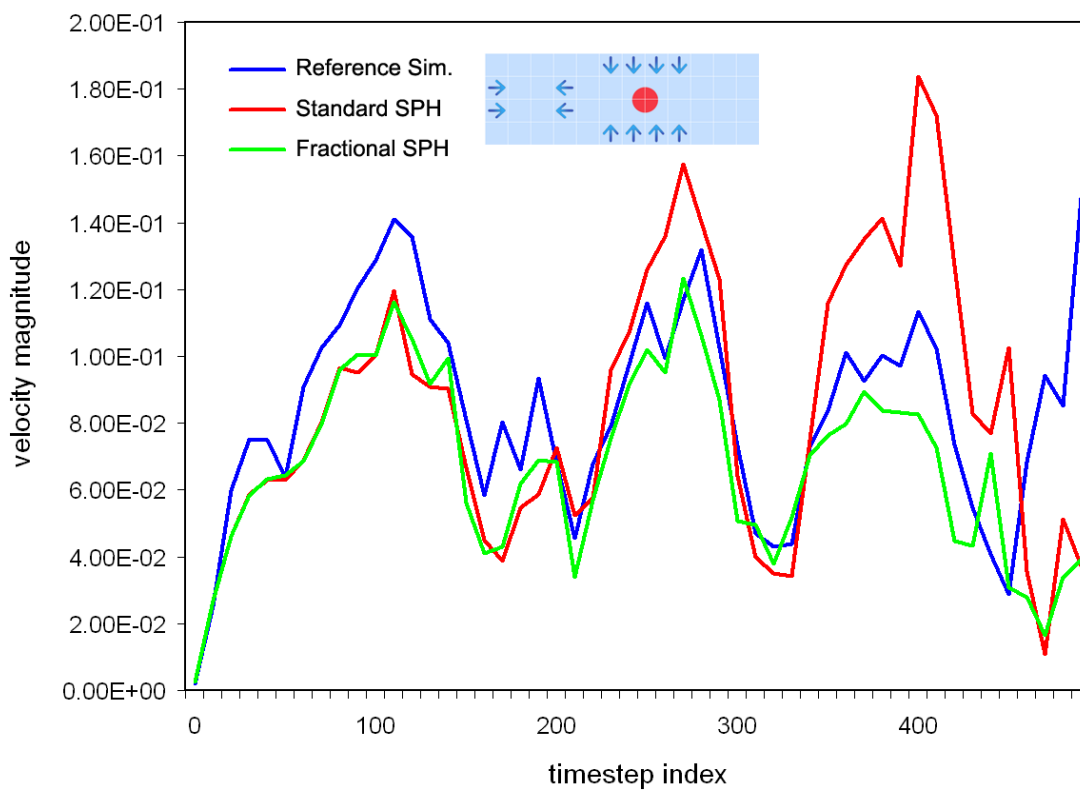


Figure 8: The plot shows the velocity magnitudes of the region marked with the red disc, over a simulation of 500 timesteps, for 2D simulations. The blue, red and green lines represent the simulations of high resolution standard SPH, low resolution standard SPH and low resolution Fractional SPH, respectively. The region marked with red disc is rich in flow collisions.

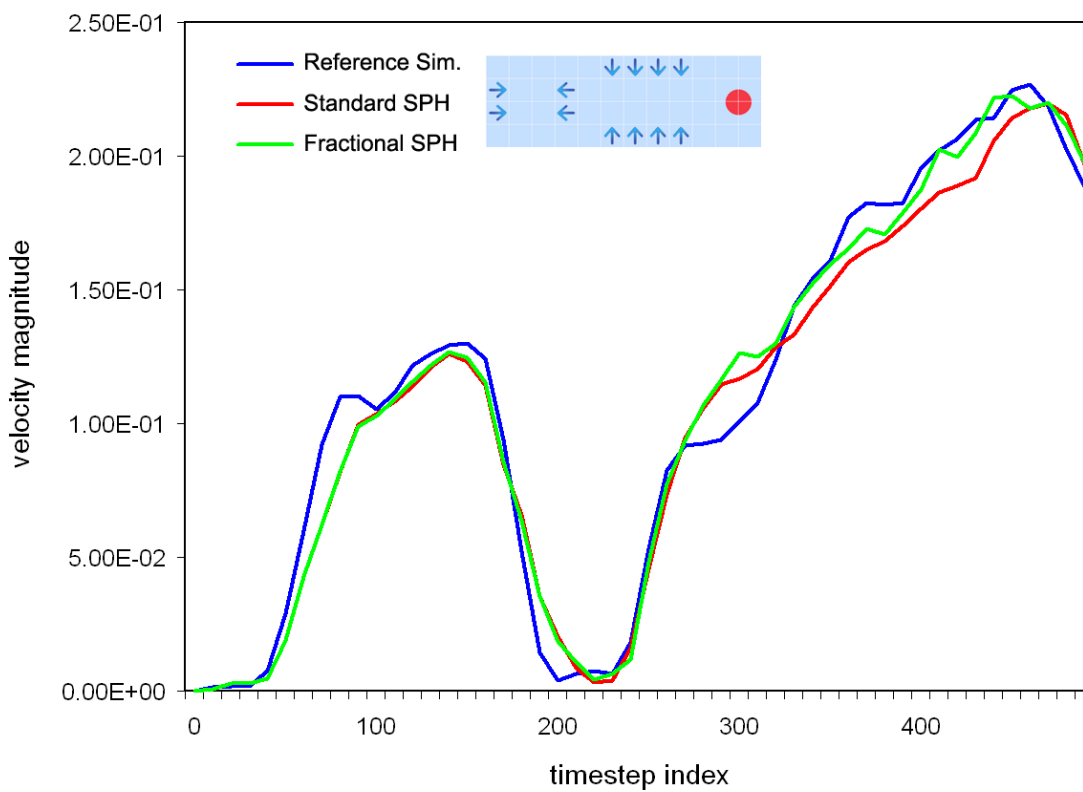


Figure 9: The plot shows the velocity magnitudes of the region marked with the red disc, over a simulation of 500 timesteps, for 2D simulations. The blue, red and green lines represent the simulations of high resolution standard SPH, low resolution standard SPH and low resolution Fractional SPH, respectively. The region marked with red disc is poor in flow collisions.

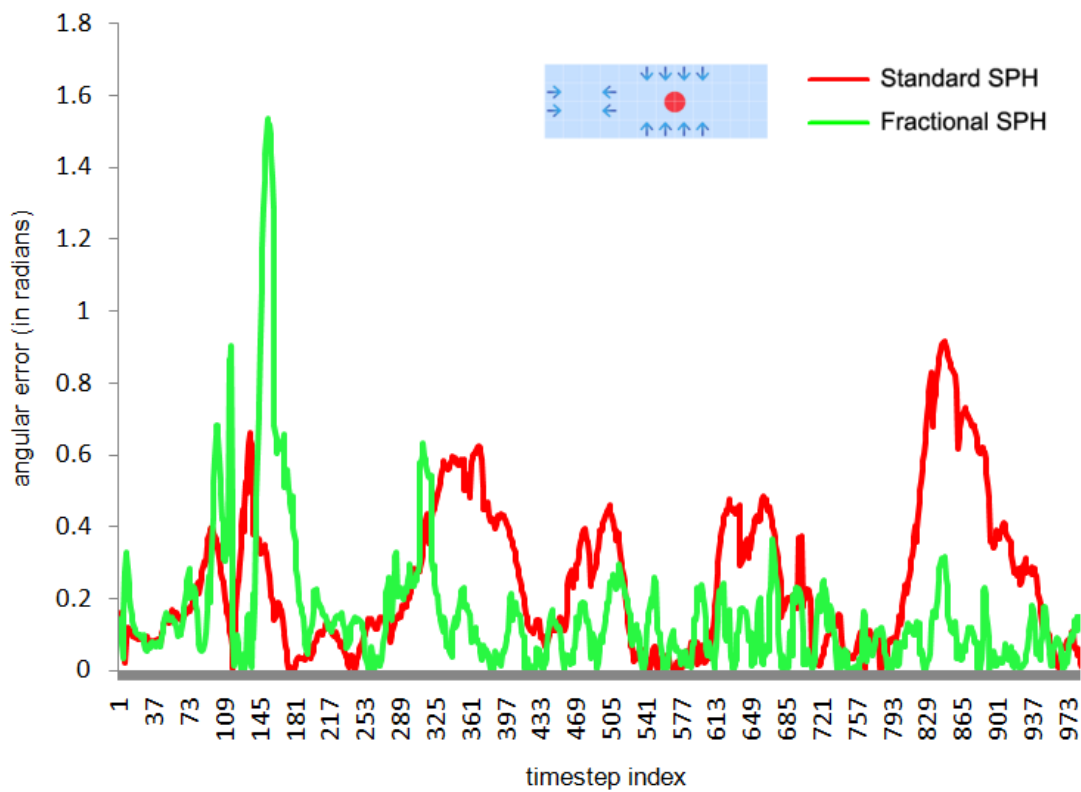


Figure 10: The plot shows the error rates in velocity directions of the region marked with the red disc, over a simulation of 1000 timesteps, in 3D simulations. The red and green lines represent the simulations of low resolution standard SPH and low resolution Fractional SPH compared against higher resolution standard SPH, respectively. The region marked with the red disc is rich in flow collisions.

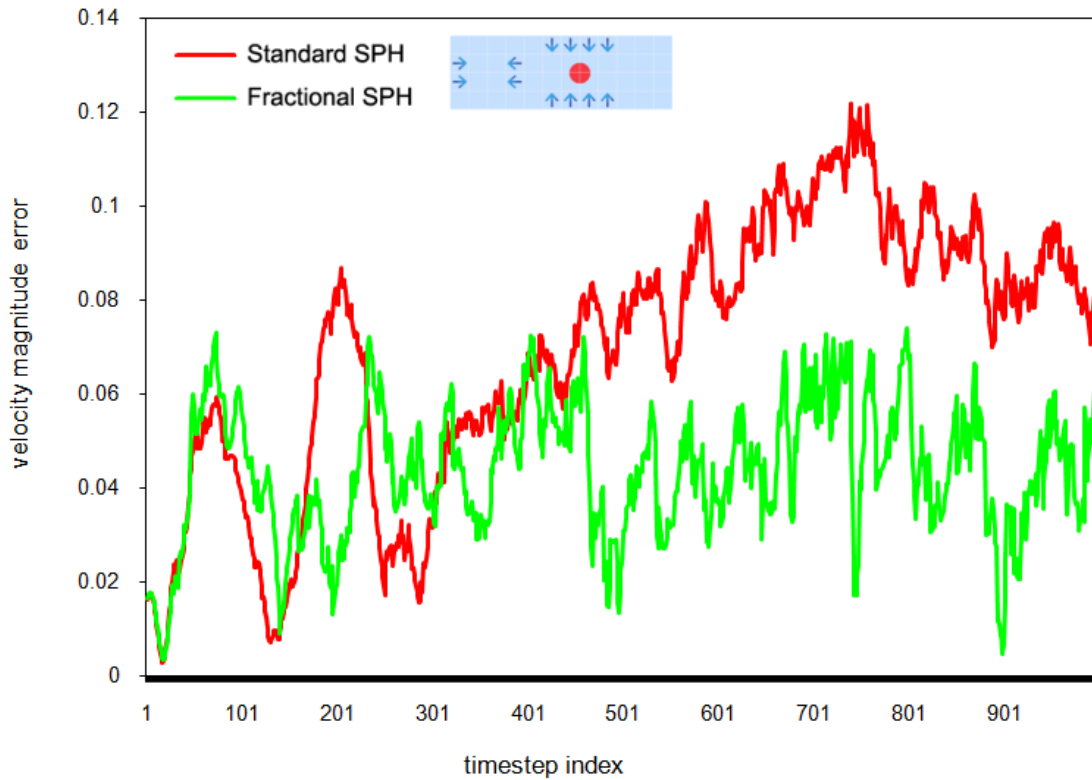


Figure 11: The plot shows the velocity magnitudes of the region marked with the red disc, over a simulation of 1000 timesteps, in 3D simulations. The red and green lines represent the simulations of low resolution standard SPH and low resolution Fractional SPH compared against higher resolution standard SPH, respectively. The region marked with red disc is rich in flow collisions.

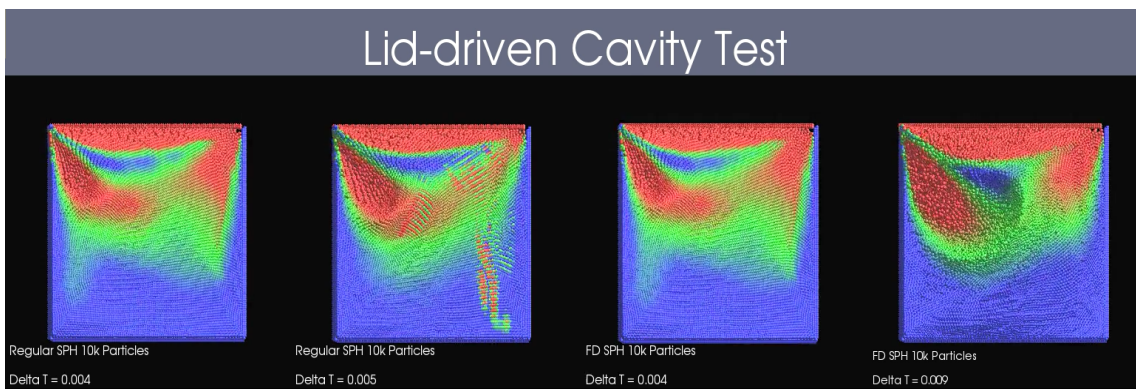


Figure 12: Lid-driven cavity test for comparing the stability of standard SPH and Fractional SPH simulations.

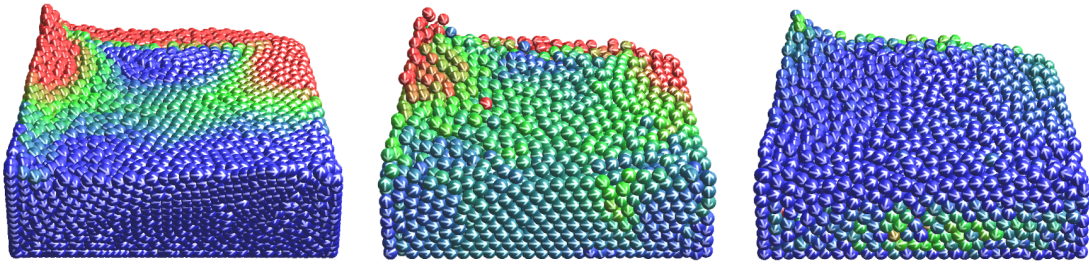


Figure 13: Average velocities and velocity directions obtained in the Shear Driven Cavity Test with different SPH simulations: 21K standard SPH (left), 6K Fractional SPH (center) and 6K standard SPH (right). Colors red, green and blue represent high, medium and low velocities respectively. The color distribution and regional velocity directions obtained with the Fractional SPH simulation are very similar to the ones in the high resolution reference simulation. This was not the case for the standard SPH in the same low resolution.

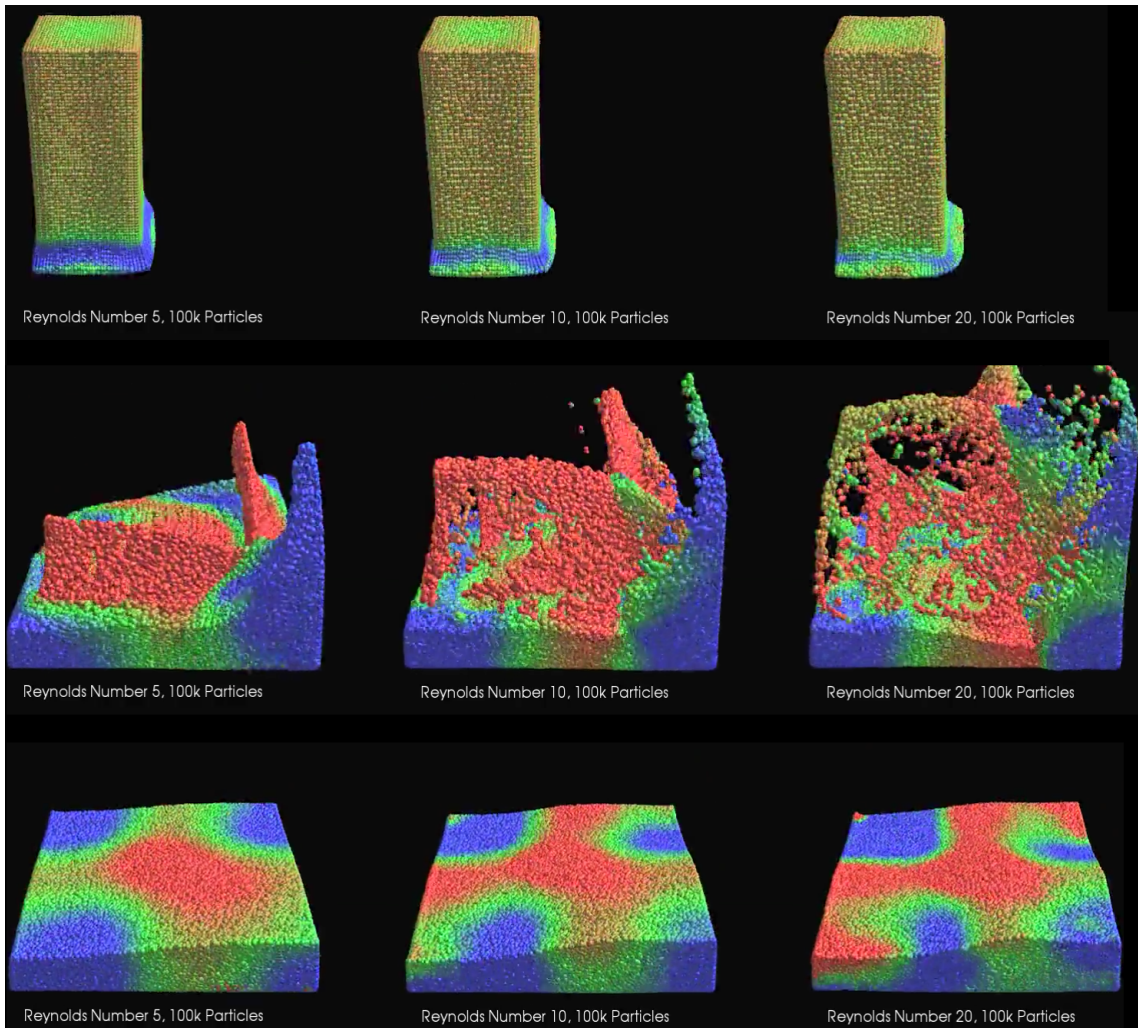


Figure 14: Dam break test using Fractional SPH, which shows the viscosity behavior of fluids with various Reynolds numbers.